Available online at www.sciencedirect.com
ScienceDirect
Journal of the European Ceramic Society 27 (2007) 3005–3010
www.elsevier.com/locate/jeurceramsoc

Effects of structural characteristics on microwave dielectric properties of $(1-x)Ca_{0.85}Nd_{0.1}TiO_3$–$xLnAlO_3$ (Ln = Sm, Er and Dy) ceramics

Eung Soo Kim *, Byung Sam Chun, Dong Ho Kang

Department of Materials Engineering, Kyonggi University, Suwon 443-760, Republic of Korea

Available online 18 December 2006

Abstract

Dependence of microwave dielectric properties on the structural characteristics of $(1-x)Ca_{0.85}Nd_{0.1}TiO_3$–$xLnAlO_3$ (Ln = Sm, Dy and Er) ceramics were investigated as a function of $LnAlO_3$ content ($0.05 \leq x \leq 0.25$). For the specimens with $SmAlO_3$, a single phase with orthorhombic perovskite was obtained through the entire composition, however, $Dy_2Ti_2O_7$ and $Er_2Ti_2O_7$ were detected as a secondary phase along with the orthorhombic perovskite phase for the specimens with $DyAlO_3$ ($x = 0.25$) and $ErAlO_3$ ($0.10 \leq x \leq 0.25$), respectively. With an increase of $LnAlO_3$ content, the dielectric constant decreased due to the smaller ionic polarizability of $LnAlO_3$ than $Ca_{0.85}Nd_{0.1}TiO_3$. The temperature coefficient of the resonant frequency (TCF) decreased with $LnAlO_3$ content resulted from an increase of oxygen octahedral distortion.

Keyword: $Ca_{0.85}Nd_{0.1}TiO_3$; Perovskites, Dielectric properties, X-ray methods

1. Introduction

With the rapid progress of microwave integrated circuits for wireless telecommunications, it has been required the microwave dielectric materials with the predictable dielectric properties of a high dielectric constant (K), a high quality factor ($Q = 1/\tan\delta$), and a nearly zero temperature coefficient of the resonant frequency (TCF). Microwave dielectric properties of $CaTiO_3$-based materials have been investigated, because of their high dielectric constant. However, TCF is too large to apply the devices. Much attention has been paid to improve their microwave dielectric properties with La^{3+}, Nd^{3+}, and Sm^{3+} substitution for Ca^{2+}.[1–3] Even though such substitution is done, TCF is still positive.

Recently, considerable efforts have been done to adjust the TCF of Ca-based materials by the formation of solid solutions of two or more compounds having negative and positive TCF values.[4,5] However, the affecting factors on TCF of microwave dielectrics should be studied to control and predict the microwave dielectric properties of materials.

The change of K and TCF is related with the dielectric polarizabilities, temperature coefficient of dielectric constant (TCK) and structural stability of compound, respectively.[6,7] Structural stability of perovskite compound could be evaluated by electronegativity of A- and B-site ions as well as the tolerance factor of ABO_3 perovskite compound. Also, the tolerance factor calculated from the effective ionic radii is closely related to the tilting of oxygen octahedra. However, the change of TCF cannot be fully explained in terms of the tolerance factor, because the effective ionic size in the center of the oxygen octahedra is changed with tilting, as reported by Shannon.[8] Also TCF of dielectric materials with tilted oxygen octahedra could be explained by the bond valence which is independent on effective ionic size.[9] As the bond valence was calculated from the average bond length of crystal structure, the dependence of TCF on the bond valence could be applied if the individual bond lengths were similar to the average bond length of oxygen octahedra. Therefore, for the remarkable change of individual bond lengths of oxygen octahedra, the tilting of oxygen octahedra could be quantitatively evaluated by the octahedral distortion, which is independent on effective ionic size,[8] so that, the octahedral distortion could be applied to explain the TCF of dielectric materials with perovskite structure.

In our previous report,[10] $(Ca_{0.85}Nd_{0.10})TiO_3$ with orthorhombic perovskite structure showed high dielectric constant and

* Corresponding author. Tel.: +82 31 249 9764; fax: +82 31 244 6300.
E-mail address: eskim@kyonggi.ac.kr (E.S. Kim).

0955-2219/$ – see front matter © 2006 Elsevier Ltd. All rights reserved.
doi:10.1016/j.jeurceramsoc.2006.11.026

good Qf value, even though TCF was too large, while $LnAlO_3$ (Ln = Sm, Dy and Er)[11] with same or distorted perovskite structure showed a negative value of TCF.

In this study, the microwave dielectric properties and crystal structure of the $(1-x)Ca_{0.85}Nd_{0.10}TiO_3$–$xLnAlO_3$ (Ln = Sm, Dy and Er) system were investigated as a function of the amount of $LnAlO_3$ ($0.05 \leq x \leq 0.25$). Dependence of dielectric constant on the dielectric polarizability and the dependence of TCF on the octahedral distortion of oxygen octahedra were also discussed.

2. Experimental procedure

$CaCO_3$, Nd_2O_3, Sm_2O_3, Dy_2O_3, Er_2O_3, TiO_2, and Al_2O_3 powders with reagent-grade were used as starting materials. They were weighed according to the compositions of $Ca_{0.85}Nd_{0.10}TiO_3$, $SmAlO_3$, $DyAlO_3$ and $ErAlO_3$, and then milled with ZrO_2 balls for 24 h in distilled water. Powders with a composition of $Ca_{0.85}Nd_{0.10}TiO_3$ were calcined at 1100 °C for 3 h, while powders with a composition of $SmAlO_3$ were calcined at 1400 °C for 3 h and powders with a composition of $DyAlO_3$ and $ErAlO_3$ were calcined at 1450 °C for 24 h. These calcined powders were mixed according to the formula of $(1-x)Ca_{0.85}Nd_{0.10}TiO_3$–$xLnAlO_3$ (Ln = Sm, Dy and Er, $0.05 \leq x \leq 0.25$). The mixed powders were milled again with ZrO_2 balls for 24 h in distilled water and then dried. The dried powders were pressed into 10 mm diameter disk at 1500 kg/cm^2 isostatically. These pellets were sintered at 1400 °C for 4 h in air.

Crystalline phases of the specimens were identified with the powder X-ray diffraction patterns (D/Max-3C, Rigaku, Japan). From the Rietveld refinements of X-ray diffraction patterns, the lattice parameters and unit cell volume of the sintered specimens were determined, and the bond lengths between A-/B-site ions and oxygen ions were obtained. Microstructure was observed using a scanning electron microscope (Hitachi S-4200, Japan). The compositions were analyzed by energy dispersive spectrometer (Hitachi S-4200, Japan). The dielectric constant, unloaded Q value at frequencies of 5–7 GHz were measured by the post-resonant method developed by Hakki and Coleman.[12] TCF was measured by the cavity method[13] at frequencies of 9–11 GHz and the temperature range of 25–80 °C.

From the lattice parameters of orthorhombic perovskite structure, the individual bond length of oxygen octahedra was obtained in the following equations:

$$R_x = R_y = \frac{\sqrt{a^2 + c^2}}{2} \tag{1}$$

$$R_z = \frac{b}{2} \tag{2}$$

where R_x, R_y, and R_z are the individual bond length of x-, y-, and z-axes in oxygen octahedra, and a, b, and c are the lattice parameters of a-, b-, and c-axes in orthorhombic perovskite, respectively. From the individual bond length of oxygen octahedra, the octahedral distortion (Δ) of orthorhombic perovskite was calculated in the following equation[8]:

$$\Delta = \frac{1}{6}\sum\left\{\frac{R_i - \bar{R}}{\bar{R}}\right\}^2 \tag{3}$$

where R_i is the individual bond length and R is the average bond length of oxygen octahedral.

3. Results and discussion

Fig. 1 shows the X-ray diffraction patterns of $(1-x)Ca_{0.85}Nd_{0.10}TiO_3$–$xLnAlO_3$ (Ln = Sm, Dy and Er, $0.05 \leq x \leq 0.25$) ceramics sintered at 1400 °C for 4 h. For the specimens with $SmAlO_3$, a single phase with orthorhombic perovskite was obtained through the entire composition, however, $Dy_2Ti_2O_7$ and $Er_2Ti_2O_7$ were detected as a secondary phase along with the orthorhombic perovskite phase for the specimens with $DyAlO_3$ ($x = 0.25$) and $ErAlO_3$ ($0.10 \leq x \leq 0.25$), respectively. These results were consistent with the stability of the perovskite structure which could be evaluated by the tolerance factor and

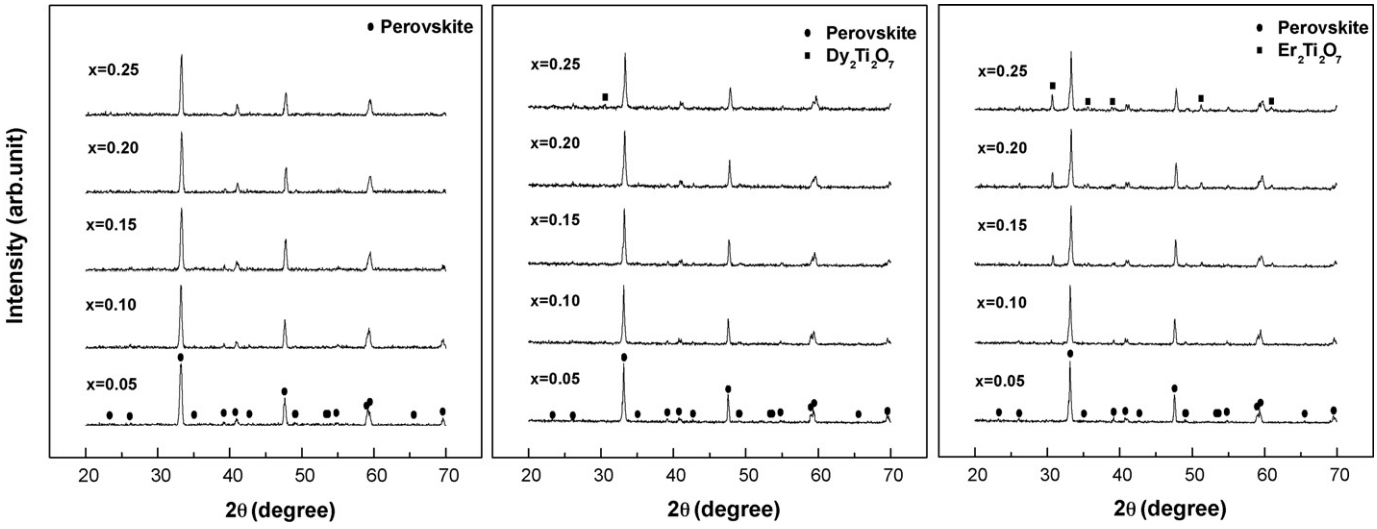

Fig. 1. X-ray diffraction patterns of $(1-x)Ca_{0.85}Nd_{0.10}TiO_3$–$xLnAlO_3$ (Ln = Sm, Dy and Er) specimens sintered at 1400 °C for 4 h.

electronegativity differences.[14] Due to the smaller ionic size of Al^{3+}ion (0.535 Å)[8] than that of Ti^{4+} ion (0.605 Å)[8] for B-site ion, and the smaller ionic size of Ln^{3+} ion (Sm = 1.079 Å, Dy = 1.027 Å, Er = 1.004 Å)[8] than the average ionic size of $(Ca_{0.85}Nd_{0.10})^{2+}$ (1.2499 Å)[8] for A-site, the tolerance factor of the specimens with $SmAlO_3$ was larger than those with $DyAlO_3$ and $ErAlO_3$. Also, the average electronegativity differences of the specimens with $SmAlO_3$ was larger than those with $DyAlO_3$ and $ErAlO_3$, which was resulted from the smaller electronegativity of Sm^{3+} ion (1.17) than those with Dy^{3+} ion (1.22) and Er^{3+} ion (1.24).[15]

Within the solid solution range, the unit cell volume of the specimens was decreased as the $LnAlO_3$ (Ln = Sm, Dy and Er) content was increased, as shown in Fig. 2. Unit-cell volume of the specimens with $SmAlO_3$ was larger than those with $DyAlO_3$ and $ErAlO_3$, which was due to the larger ionic size of Sm^{3+} (1.079 Å) than that of Dy^{3+} (1.027 Å) and Er^{3+} (1.004 Å)[8]. Density of the specimens with $SmAlO_3$ showed a maximum value at $x = 0.15$, while those with $DyAlO_3$ and/or $ErAlO_3$ decreased as the results of the increase of $DyAlO_3$ and/or $ErAlO_3$ content, respectively. Relative densities were higher than 96% of theoretical values for all of the specimens.

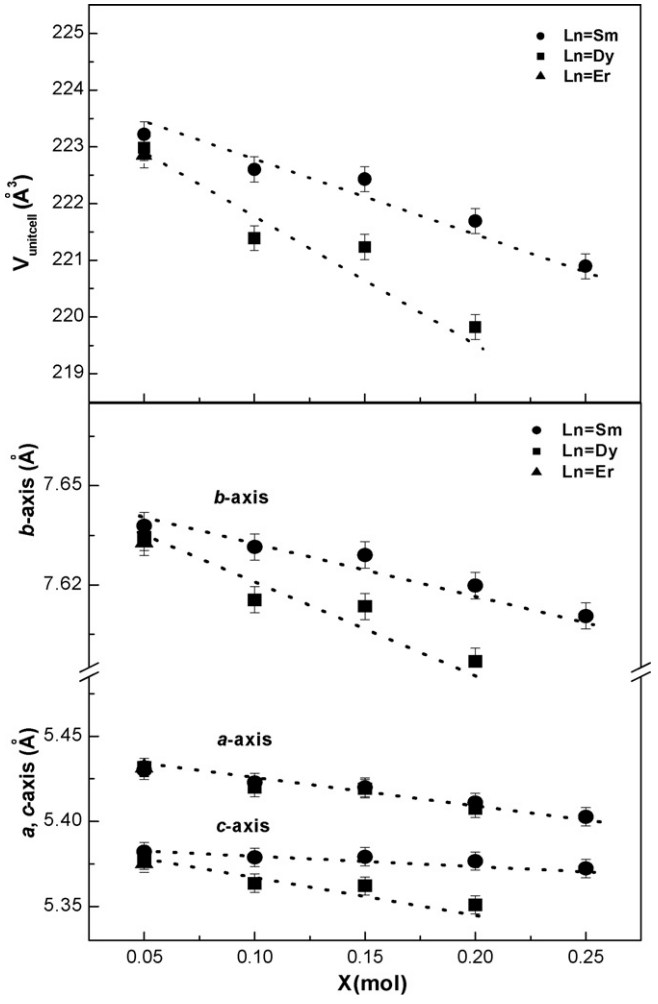

Fig. 2. Lattice parameters and unit-cell volume of $(1-x)Ca_{0.85}Nd_{0.10}TiO_3$–$xLnAlO_3$ (Ln = Sm, Dy and Er) specimens sintered at 1400 °C for 4 h.

Table 1
Microwave dielectric properties of $Ln_2Ti_2O_7$ (Ln = Dy and Er) ceramics

Compound	*K*	*Q*	Structure
$Dy_2Ti_2O_7$	57.1	301	Cubic pyrochlore
$Er_2Ti_2O_7$	58.8	230	Cubic pyrochlore
$Er_2Ti_2O_7$[a]	61	200	Cubic pyrochlore

[a] Mater. Res. Bull. 37 (2002) 2077.

Fig. 3 shows SEM micrographs of the specimens sintered at 1400 °C for 4 h. The grain size of the specimens with $SmAlO_3$ increased slightly with $SmAlO_3$ content up to 0.15 mol, and then decreased drastically after further addition. However, the grain size decreased with $DyAlO_3$ and/or $ErAlO_3$ content, and the secondary phase was detected for the specimens with $DyAlO_3$ and/or $ErAlO_3$. To confirm the secondary phase of $0.75Ca_{0.85}Nd_{0.10}TiO_3$–$0.25LnAlO_3$ (Ln = Dy and Er), the back-scattered electron images and EDS analysis were performed, as shown in Fig. 4. From the EDS results, the cubic pryochlore $Dy_2Ti_2O_7$ phase (D) and $Er_2Ti_2O_7$ phase (E) were detected for the specimens with $DyAlO_3$ and $ErAlO_3$, respectively. These results are agreed with XRD patterns of Fig. 1.

Fig. 5 shows the microwave dielectric properties (*K*, Qf) of $(1-x)Ca_{0.85}Nd_{0.10}TiO_3$–$xLnAlO_3$ (Ln = Sm, Dy and Er) specimens sintered at 1400 °C for 4 h. Quality factor (Qf) of the specimens with $SmAlO_3$ increased with $SmAlO_3$ content up to $x = 0.15$, and then decreased due to the changes of density and grain size as there was no detection of secondary phase, moreover, Qf of the specimens with $DyAlO_3$ and $ErAlO_3$ decreased with $DyAlO_3$ and $ErAlO_3$ content due to the decrease of density and the formation of secondary phase, $Dy_2Ti_2O_7$ and $Er_2Ti_2O_7$, which has a lower *Q* value than that of $Ca_{0.85}Nd_{0.10}TiO_3$–$LnAlO_3$ (Ln = Sm, Dy and Er) solid solution, as shown in Table 1.

Dielectric constant (*K*) was significantly dependent upon the relative density and ionic polarizability at microwave frequencies. Effects of density on the dielectric constant could be neglected because the relative density of the specimens was higher than 96% of X-ray density. The dielectric constant (*K*) of the specimens decreased with $LnAlO_3$ (Ln = Sm, Dy and Er) content due to the smaller dielectric polarizability of $SmAlO_3$ (11.56 Å), $DyAlO_3$ (10.89 Å) and $ErAlO_3$ (10.63 Å) than $Ca_{0.85}Nd_{0.15}TiO_3$ (12.15 Å).[16] Moreover, *K* of the specimens with $SmAlO_3$ was higher than those of specimens with $DyAlO_3$ and $ErAlO_3$. These results could be attributed to the larger ionic polarizability of Sm^{3+} (4.74 Å) than those of Dy^{3+} (4.07 Å) and Er^{3+} (3.81 Å) (Table 2).[16]

Table 2
EDS results of $0.75Ca_{0.85}Nd_{0.10}TiO_3$–$0.25LnAlO_3$ (Ln = Dy and Er) specimens sintered at 1400 °C for 4 h

(a) Grain D			(b) Grain E		
Element	Element (%)	Atomic (%)	Element	Element (%)	Atomic (%)
O	17.68	74.04	O	19.27	73.56
Dy	22.17	12.87	Er	23.98	13.22
Ti	60.15	13.10	Ti	56.75	13.22

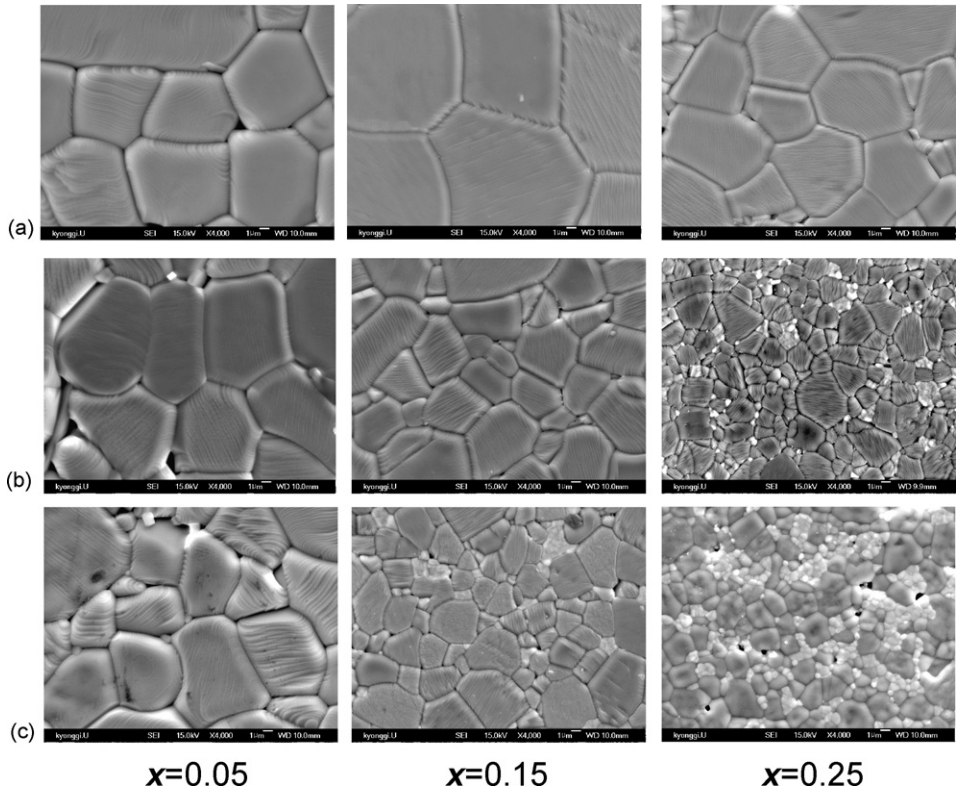

Fig. 3. SEM micrographs of $(1-x)Ca_{0.85}Nd_{0.10}TiO_3$–$xLnAlO_3$ specimens sintered at 1400 °C for 4 h: (a) Ln = Sm; (b) Ln = Dy; (c) Ln = Er.

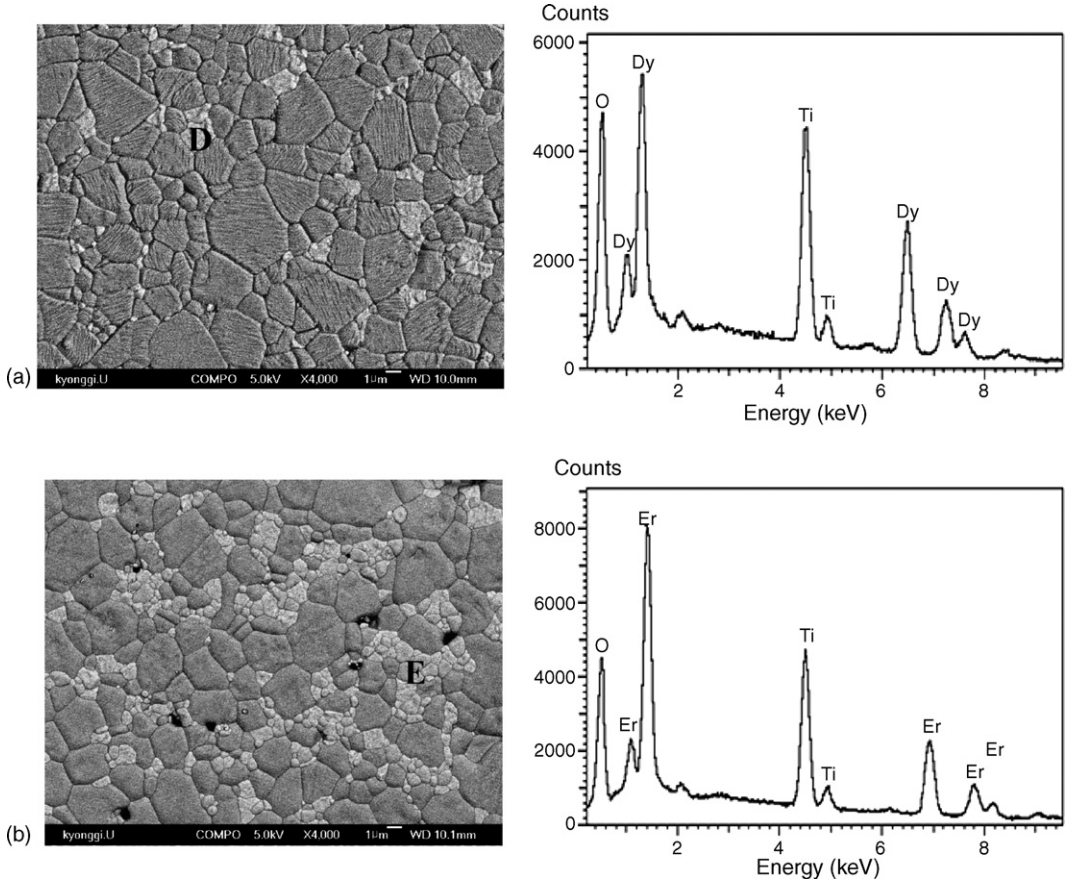

Fig. 4. Back-scattered electron images of $0.75Ca_{0.85}Nd_{0.10}TiO_3$–$0.25LnAlO_3$ specimens sintered at 1400 °C for 4 h: (a) Ln = Dy; (b) Ln = Er.

Table 3
Octahedral distortion and TCF of $(1-x)Ca_{0.85}Nd_{0.10}TiO_3$–$xLnAlO_3$ (Ln = Sm, Dy and Er) ceramics sintered at 1400 °C for 4 h

Ln	x	a (Å)	b (Å)	c (Å)	R_x, R_y (Å)	R_z (Å)	Average R_{B-O}	Distortion, Δ ($\times 10^6$)	TCF (ppm/°C)
Sm	0.05	5.4300	7.6392	5.3822	3.8227	3.8196	1.9108	0.1492	107.28
	0.10	5.4229	7.6315	5.3788	3.8190	3.8158	1.9090	0.1605	81.06
	0.15	5.4200	7.6291	5.3792	3.8181	3.8146	1.9085	0.1963	52.37
	0.20	5.4111	7.6199	5.3767	3.8141	3.8099	1.9064	0.2656	12.83
	0.25	5.4027	7.6107	5.3722	3.8095	3.8054	1.9041	0.2629	−5.53
Dy	0.05	5.4317	7.6345	5.3771	3.8216	3.8173	1.9101	0.2797	90.66
	0.10	5.4200	7.6155	5.3636	3.8126	3.8078	1.9055	0.3622	54.20
	0.15	5.4191	7.6135	5.3622	3.8118	3.8068	1.9051	0.3910	29.82
	0.20	5.4077	7.5968	5.3510	3.8038	3.7984	1.9010	0.4484	2.43
Er	0.05	5.4315	7.6329	5.3754	3.8209	3.8165	1.9097	0.2965	87.23

Table 3 summarized the oxygen octahedral distortion of $Ca_{0.85}Nd_{0.10}TiO_3$–$LnAlO_3$ (Ln = Sm, Dy and Er) ceramics obtained from Eqs. (1)–(3), and TCF of the specimens measured at 9–11 GHz in the temperature range from 25 to 80 °C. With the increase of $LnAlO_3$ content, the distortion of oxygen octahedron increased and TCF was decreased. The strong dependence of thermal stability (TCF) on the octahedral distortion of $Ca_{0.85}Nd_{0.10}TiO_3$–$LnAlO_3$ (Ln = Sm, Dy and Er) ceramics was shown in Fig. 6. Therefore, TCF of perovskite compound could be evaluated and predicted by the degree of octahedral distortions if the perovskite compound has the tilted oxygen octahedra.

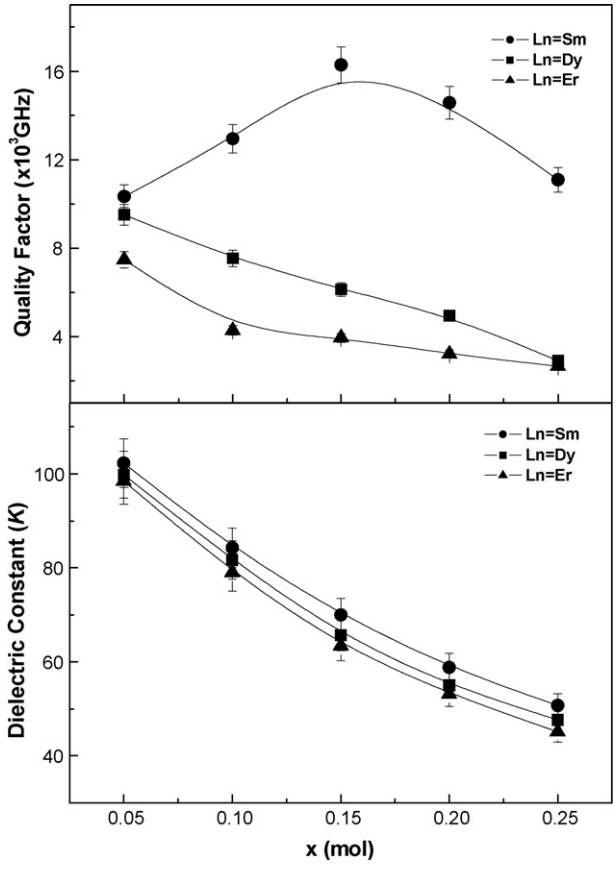

Fig. 5. Microwave dielectric properties of $(1-x)Ca_{0.85}Nd_{0.10}TiO_3$–$xLnAlO_3$ (Ln = Sm, Dy and Er) specimens sintered at 1400 °C for 4 h.

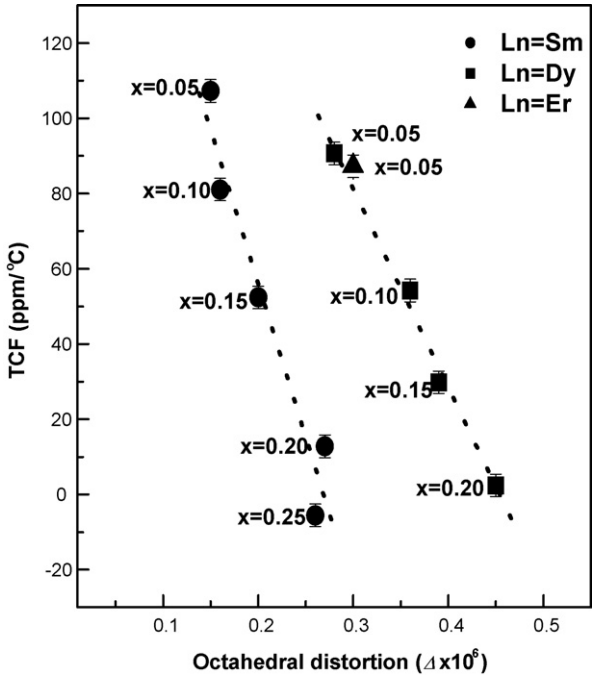

Fig. 6. Dependence of TCF on octahedral distortion of $(1-x)Ca_{0.85}Nd_{0.10}TiO_3$–$xLnAlO_3$ (Ln = Sm, Dy and Er) specimens sintered at 1400 °C for 4 h.

4. Conclusion

Dielectric constant (K) decreased with $LnAlO_3$ (Ln = Sm, Dy and Er) content due to the smaller dielectric polarizability of $LnAlO_3$ than $Ca_{0.85}Nd_{0.15}TiO_3$. Quality factor (Qf) of the specimens with $SmAlO_3$ increased with $SmAlO_3$ content up to $x = 0.15$, and then decreased, while those of the specimens with $DyAlO_3$ and $ErAlO_3$ was decreased with $DyAlO_3$ and $ErAlO_3$ content due to the decrease of density and the formation of secondary phase, $Dy_2Ti_2O_7$ and $Er_2Ti_2O_7$.

Thermal stability (TCF) of the specimens was strongly depended on the degree of oxygen octahedral distortion (Δ).

Typically value of $K = 58.85$, Qf = 14,574 GHz, TCF = 12.83 ppm/°C were obtained for $0.80Ca_{0.85}Nd_{0.10}TiO_3$–$0.20SmAlO_3$ specimens sintered at 1400 °C for 4 h.

Acknowledgements

This work was supported by LG Innotek and the Ministry of Commerce, Industry and Energy. Authors would deeply appreciate to Prof. R.J. Cernik at University of Manchester in UK and Prof. H.S. Shin at Kaya Univeristy in Korea for helpful discussions of the Rietveld refinements of X-ray diffraction patterns.

References

1. Kim, I. S., Jung, W. H., Inaguma, Y., Nakamura, T. and Itoh, M., Dielectric properties of A-site deficient perovskite-type lanthanum–calcium–titanium oxide solid solution system $[(1-x)La_{2/3}TiO_3$–$xCaTiO_3$ $(0.1 \leq x \leq 0.96)$. *Mater. Res. Bull.*, 1995, **30**(3), 307–316.
2. Yoshida, M., Hara, N., Takada, T. and Seki, A., Structure and dielectric properties $(Ca_{1-x}\ Nd_{2x/3})TiO_3$. *Jpn. J. Appl. Phys.*, 1997, **36**(11), 6818–6823.
3. Kim, W. S., Kim, E. S. and Yoon, K. H., Effect of Sm^{3+} substitution on dielectric properties of $Ca_{1-x}Sm_{2x/3}TiO_3$ ceramics at microwave frequencies. *J. Am. Ceram. Soc.*, 1999, **82**(8), 2111–2115.
4. Kim, W. S., Yoon, K. H. and Kim, E. S., Microwave dielectric characteristics of $Ca_{2/5}Sm_{2/5}TiO_3$–$Li_{1/2}Nd_{1/2}TiO_3$ ceramics. *Jpn. J. Appl. Phys.*, 2000, **39**(9B), 5650–5653.
5. Kim, W. S., Yoon, K. H. and Kim, E. S., Far-infrared reflectivity spectra of $CaTiO_3$–$Li_{1/2}Sm_{1/2}TiO_3$ microwave dielectrics. *Mater. Res. Bull.*, 1999, **34**(14/15), 2309–2317.
6. Colla, E. L., Reaney, I. M. and Setter, N., Effect of structural changes in complex perovskites on the temperature coefficient of the relative permittivity. *J. Appl. Phys.*, 1993, **74**, 3414–3425.
7. Reaney, I. M., Colla, E. L. and Setter, N., Dielectric and structural characteristics of Ba- and Sr-based complex perovskites as a function of tolerance factor. *Jpn. J. Appl. Phys.*, 1994, **33**(7A), 3984–3990.
8. Shannon, R. D., Revised Effective ionic radii and systematic studies of interatomic distances in halides and chalcogenides. *Acta Cryst. A*, 1976, **32**, 751–767.
9. Park, H. S., Yoon, K. H. and Kim, E. S., Relationship between the bond valence and the temperature coefficient of the resonant frequency in the complex perovskite $(Pb_{1-x}Ca_x)$ $[Fe_{0.5}(Nb_{1-y}Ta_y)_{0.5}]O_3$. *J. Am. Ceram. Soc.*, 2001, **84**(1), 99–103.
10. Kim, E. S., Chun, B. S., Bang, K. S. and Kim, J. C., Microwave dielectric properties of $Ca_{1-x}Nd_{2x/3}TiO_3$ ceramics. *J. Kor. Ceram. Soc.*, 2001, **38**(7), 672–677.
11. Cho, S. Y., Kim, I. T. and Hong, K. S., Microwave dielectric properties and applications of rare-earth aluminates. *J. Mater. Res.*, 1999, **14**(8), 114–119.
12. Hakki, B. W. and Coleman, P. D., A dielectric resonator method of measuring inductive capacities in the millimeter range. *IRE Trans. Microwave Theory Tech.*, 1970, **MTT18**, 476–485.
13. Nishikawa, T., Wakino, K., Tamura, H., Tanaka, H. and Ishikawa, Y., Precise measurement method for temperature coefficient of microwave dielectric resonator material. *IEEE MTT-S Int. Microwave Symp. Dig.*, 1987, 277–280.
14. Halliyal, A., Kumar, U., Newnham, R. E. and Cross, L. E., Stabilization of the perovskite phase and dielectric properties of ceramics in the $Pb(Zn_{1/3}Nb_{2/3})O_3$–$BaTiO_3$ system. *Am. Ceram. Soc. Bull.*, 1987, **66**(4), 671–676.
15. Pauling, L., *The Nature of Chemical Bonds*. Cornell University Press, Cornell, NY, 1960.
16. Shannon, R. D., Dielectric polarizabilities of ions in oxides and fluorides. *J. Appl. Phys.*, 1993, **73**(1), 348–366.